

71-01587

FURTHER STUDIES OF PROPELLANT SLOSHING UNDER LOW-GRAVITY CONDITIONS

by

Franklin T. Dodge

FINAL REPORT

Contract No. NAS8-24022

Control No. DCN 1-9-75-10061(3F)

SwRI Project 02-2578

Prepared for

National Aeronautics and Space Administration

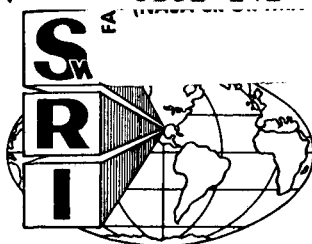
George C. Marshall Space Flight Center

Marshall Space Flight Center, Alabama 35812

March 1971

N72-14783 (NASA-CR-119892) FURTHER STUDIES OF
PROPELLANT SLOSHING UNDER LOW-GRAVITY
CONDITIONS Final Report F.T. Dodge
Unclas (Southwest Research Inst.) Mar. 1971 23 p
11871 CSCL 21I

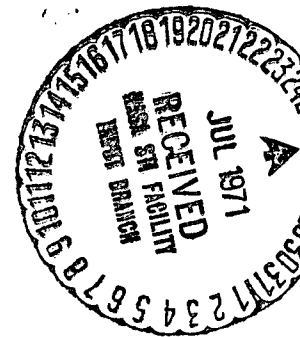
G3/27



SOUTHWEST RESEARCH INSTITUTE
SAN ANTONIO HOUSTON

Reproduced by
**NATIONAL TECHNICAL
INFORMATION SERVICE**
U S Department of Commerce
Springfield VA 22151

148
SOUTHWEST RESEARCH INSTITUTE
Post Office Drawer 28510, 8500 Culebra Road
San Antonio, Texas 78228



FURTHER STUDIES OF PROPELLANT SLOSHING UNDER LOW-GRAVITY CONDITIONS

by

Franklin T. Dodge

FINAL REPORT

Contract No. NAS8-24022

Control No. DCN 1-9-75-10061(3F)

SwRI Project 02-2578.

Prepared for

National Aeronautics and Space Administration
George C. Marshall Space Flight Center
Marshall Space Flight Center, Alabama 35812

March 1971

Approved:

H. Norman Abramson, Director
Department of Mechanical Sciences

PREFACE

Two separate phases of propellant sloshing under low-gravity conditions were investigated during this project. Results of the first phase, an experimental and analytical study of sloshing in rectangular tanks, have been reported previously in Technical Report No. 1, January 1970. A summary of Technical Report No. 1 is presented as the Appendix to this Final Report. Details of the second phase, which is comprised of an analytical study of sloshing in ellipsoidal tanks, are included as the major portion of this Final Report.

The SwRI Project Manager was Dr. Franklin T. Dodge. Mr. Luis R. Garza contributed substantially to the experimental portion of the research, and Dr. Wen-Hwa Chu made several valuable suggestions concerning the analytical approach.

The entire program was made possible by the continuing efforts of the NASA-MSFC technical monitors: Mr. Robert S. Ryan, Mr. Frank Bugg, and Mr. Harry Buchanan.

ABSTRACT

A variational integral is formulated from Hamilton's principle and is proved to be equivalent to the usual differential equations of low-gravity sloshing in ellipsoidal tanks. It is shown that for a zero-degree contact angle the contact line boundary condition corresponds to the "stuck" condition, a result that is due to the linearization of the equations and the ambiguity in the definition of the wave height at the wall.

The variational integral is solved by a Rayleigh-Ritz technique. Results for slosh frequency when the free surface is not "bent-over" compare well with previous numerical solutions. When the free surface is "bent over," however, the results for slosh frequency are considerably larger than those predicted by previous finite-difference, numerical approaches; the difference may be caused by the use of a zero degree contact angle in the present theory in contrast to the nonzero contact angle used in the numerical approaches.

TABLE OF CONTENTS

	<u>Page</u>
LIST OF FIGURES	<i>vi</i>
LIST OF SYMBOLS	<i>vii</i>
I. INTRODUCTION	1
II. EQUILIBRIUM FREE SURFACE	2
III. SLOSHING ANALYSIS	6
A. Basic Equations	6
B. Contact Line Condition	10
IV. SOLUTION OF EQUATIONS	12
A. Rayleigh-Ritz Technique	12
B. Trial Functions and Results	13
V. CONCLUSIONS	15
VI. REFERENCES	16
APPENDIX—SUMMARY OF “LOW GRAVITY SLOSHING IN RECTANGULAR TANKS” . . .	17

PRECEDING PAGE BLANK NOT FILMED

LIST OF FIGURES

<u>Figure</u>		<u>Page</u>
1	Nomenclature for Equilibrium Shape of Liquid	2
2	Comparison of Approximate and Exact Theories	
	a. $N_{BO} = 10$, 75% and 12.5% Full	5
	b. $N_{BO} = 30$, 87.5% and 25% Full	5
	c. $N_{BO} = 100$, 62.5% and 37.5% Full	5
3	Normal-Tangential Coordinate System	9
4	Various Contact Line Conditions	11

LIST OF SYMBOLS

$a_k^{(n)}$	constants in Eq. (41)
A_{nm}, B_{nm}	various definite integrals
b	radius to point of vertical tangency of free surface, see Fig. 1
C	curvature of free surface
f	height of free surface above $z = 0$, see Fig. 1
F	f/r_o
g	gravity or equivalent steady axial acceleration of tank
h	location of r, z coordinate system above center of tank, see Fig. 1
H	h/r_o
I	variational integral
J_1	Bessel function of first kind of order one
ℓ	semi-axis of tank, see Fig. 1
L	ℓ/r_o
N_{BO}	Bond number, $\rho g r_o^2 / \sigma$
p	liquid pressure
p_o	gas pressure
r, z, θ	cylindrical coordinate system, see Fig. 1
R, Z, θ	$r/r_o, z/r_o, \theta$, respectively
r_o	radius of tank
r_w	radius to point of intersection of free surface and tank wall, see Fig. 1
R_w	r_w/r_o
w	$z = w(r)$, equation of tank surface
W	w/r_o
α_n	constants in expansion of Φ into a series
β	defined in Eq. (12) or see Fig. 1
Γ, Γ'	constants describing contact line conditions

LIST OF SYMBOLS (Cont'd)

δ	variation symbol
$\epsilon(R, \theta)$	$\bar{\eta}\Omega/r_o$
$\bar{\eta}(r, \theta)$	slosh wave height
λ_n	parameter in Bessel function solution of $\nabla^2 \Phi = 0$
μ	defined in Eq. (13)
ρ, σ	liquid density and surface tension
$\bar{\phi}(r, \theta, z)$	velocity potential
$\Phi(R, \theta, Z)$	$\bar{\phi}/(gr_o^3)^{1/2}$
ψ	contact angle
ω	slosh natural frequency
Ω	$\omega(g/r_o)^{1/2}$
∇	Laplacian operator

I. INTRODUCTION

The study of liquid sloshing under strong capillary and weak gravity conditions, usually called low-gravity sloshing, was begun in detail with the publication in 1964 of the report [1]* by Satterlee and Reynolds, dealing with circular cylindrical tanks. By 1966, low-gravity sloshing in a circular cylindrical tank was sufficiently well understood to allow an equivalent (mathematical) mechanical model to be derived [2]. Detailed research concerning spherical and ellipsoidal tanks began somewhat later, with the delay probably caused by the knowledge that there would be considerable analytical difficulties with these geometries. Thus, it was not until early in 1968 that the present analytical work was started at SwRI to predict low-gravity sloshing behavior in an ellipsoidal tank, under the initial sponsorship of Contract NAS8-20290, and later under the sponsorship of Contract NAS8-24022, both with NASA-MSFC.

To avoid as much as possible the expected analytical trouble in satisfying exactly all the mathematical "boundary conditions" for low-gravity sloshing in spheroidal tanks, it was decided to formulate the equations of motion as an integral of the kinetic and potential energy (Hamilton's principle) and then to find the solution by a Rayleigh-Ritz approximation technique. Rattaya had shown this procedure to be satisfactory for ordinary sloshing (flat interface) in spheroidal tanks [3]. In fact, Yeh had already derived such an integral for conditions under which the free surface does not "bend over" although he presented no numerical solutions [4].

During the 3 years since this research was started, several numerical solutions of the exact differential equations of low-gravity sloshing have appeared, either for an ellipsoidal tank [5] or for a more general axisymmetric tank [6].† Thus, the numerical results of the present work are now somewhat out-of-date, especially since a completely satisfactory solution for sloshing with a "bent over" free surface has not been obtained. The present analysis is still significant, nevertheless, because several difficulties are pointed out which relate to the difficulty in obtaining correct expressions for the behavior of the slosh wave at the tank wall in the event that the contact angle is zero degrees. These difficulties are not so evident in a completely numerical treatment, where the contact angle is usually taken to be about five degrees [5, 6]. Furthermore, an approximate but easily made calculation of the equilibrium free-surface shape is presented herein; this result should be useful for making quick computations of liquid volumes or tank sizing requirements.

*Numbers in brackets refer to References listed in Section VI of this report.

†A major reason for the delay in completing the present work was the Project Manager's heavy involvement in developing the computer program described in Ref. 6.

II. EQUILIBRIUM FREE SURFACE

When gravitational forces are small, the shape of the free surface is determined by the combined influence of gravity g , surface tension σ , and contact angle ψ . Thus, the equilibrium free surface for an axisymmetric tank is a surface of revolution about the z -axis (the z -axis and the direction of gravity coincide) as shown in Figure 1.

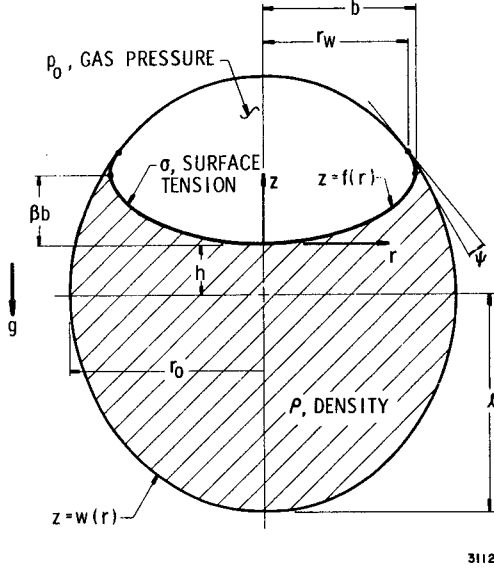


FIGURE 1. NOMENCLATURE FOR EQUILIBRIUM SHAPE OF LIQUID

Let the equation of the free surface be $z = f(r)$ and the equation of the tank shape be $z = w(r)$; both f and w may be double-valued functions. The free-surface shape is determined by the following equations [1,2]:

$$p_o - p = \sigma C \quad (1)$$

which relates the pressure jump to the curvature C of the free surface. The curvature C is

$$C = \pm \frac{d}{dr} \left\{ \frac{r(df/dr)}{[1 + (df/dr)^2]^{1/2}} \right\} \quad (2)$$

where the negative sign corresponds to the bent-over part of the surface. The liquid pressure p must satisfy the hydrostatic requirement:

$$p = p_o' - \rho g f \quad (3)$$

where p_o' is the liquid pressure at $r = z = 0$. Combining Eqs. (1), (2), and (3) gives

$$\pm \frac{\sigma}{r} \frac{d}{dr} \left\{ \frac{r(df/dr)}{[1 + (df/dr)^2]^{1/2}} \right\} - \rho g f = p_o - p_o' \quad (4)$$

The pressure difference $p_o - p_o'$ depends on the curvature at the center ($r = z = 0$). Because $f = df/dr = 0$ at $r = 0$, Eq. (4) shows that this pressure jump is

$$p_o - p_o' = 2\sigma \left(\frac{d^2 f}{dr^2} \right)_{r=0} \quad (5)$$

Thus, the governing differential equation can be obtained by combining Eqs. (4) and (5):

$$\pm \frac{\sigma}{r} \frac{d}{dr} \left\{ \frac{r(df/dr)}{[1 + (df/dr)^2]^{1/2}} \right\} - 2\sigma \left(\frac{d^2 f}{dr^2} \right)_{r=0} - \rho g f = 0 \quad (6)$$

The boundary conditions on f are

$$f = \frac{df}{dr} = 0 \quad \text{at } r = 0 \quad (7)$$

$$\frac{df}{dr} = \tan \left[\psi + \arctan \left(\frac{dw}{dr} \right) \right] \quad \text{at } r = r_w \quad (8)$$

where ψ is the angle of contact. By letting $R = r/r_o$, $F = f/r_o$, $W = w/r_o$, and $N_{BO} = \rho g r_o^2 / \sigma$, Eqs. (6), (7), and (8) can be written in nondimensional form as

$$\pm \frac{d}{R dR} \left\{ \frac{R(dF/dR)}{[1 + (dF/dR)^2]^{1/2}} \right\} - 2 \left(\frac{d^2 F}{dR^2} \right)_{R=0} - N_{BO} F = 0 \quad (9)$$

$$\left. \begin{array}{l} F = 0 \\ \frac{dF}{dR} = 0 \end{array} \right\} \text{ at } R = 0 \quad (10)$$

$$\frac{dF}{dR} = \frac{dW}{dR} \text{ at } R = R_w \quad (11)$$

and, in Eq. (11), the contact angle ψ is assumed to be zero. The tank shape is $W(R) = -H \pm L(1 - R^2)^{1/2}$, where $H = h/r_o$ and $L = \ell/r_o$ (see Fig. 1).

The nonlinear Eq. (9) cannot be solved in closed form. Furthermore, there were no computer programs to solve Eq. (9) numerically for bent-over free surfaces at the time the present work was started, although several now are available. Thus, an approximate solution was obtained. After a considerable amount of trial-and-error analysis, the following equations were found to represent the free-surface shape adequately. For the *lower part* of the surface,

$$F = F_1 = \beta B \left\{ 1 - [1 - (R/B)^2]^{1/2} \right\} \quad (12)$$

and, for the *upper, or bent-over, part* of the surface,

$$F = F_2 = \beta B + \mu B [1 - (R/B)^4]^{1/2} \quad (13)$$

The point at which F_1 is joined to F_2 is $R = B = b/r_o$, which is the nondimensional radius to the point where the surface has its vertical tangent (see Fig. 1). For surfaces that are not bent over, F_2 is not needed, and, in this case, B may be larger than R_w . The parameters β , μ , R_w , and B are determined by the boundary conditions on F and by geometric considerations.

If the surface is not bent over, then Eq. (11) is satisfied if

$$\beta = LB \left[\frac{1 - (R_w/B)^2}{1 - R_w^2} \right]^{1/2} \quad (14)$$

Requiring that the free surface must intersect the tank wall at $R = R_w$ gives the result that

$$\beta B \left\{ 1 - [1 - (R_w/B)^2]^{1/2} \right\} = -H - L(1 - R_w^2)^{1/2} \quad (15)$$

Finally, Eq. (12) must satisfy Eq. (9) at least on the average; that is, F_1 must satisfy Eq. (9) when integrated from $R = 0$ to $R = B$. This requires that

$$\frac{1}{\beta} = 1 + 0.168 B^2 N_{BO} \quad (16)$$

Equations (14), (15), and (16) allow β , B , and R_w to be calculated for a given N_{BO} and volume of liquid.

If the surface is bent over, the same procedure shows that

$$\mu R_w^2 = \frac{1}{2} (LB^3) \left[\frac{1 - (R_w/B)^4}{1 - R_w^2} \right]^{1/2} \quad (17)$$

$$\beta B + \mu B [1 - (R_w/B)^4]^{1/2} = -H + L(1 - R_w^2)^{1/2} \quad (18)$$

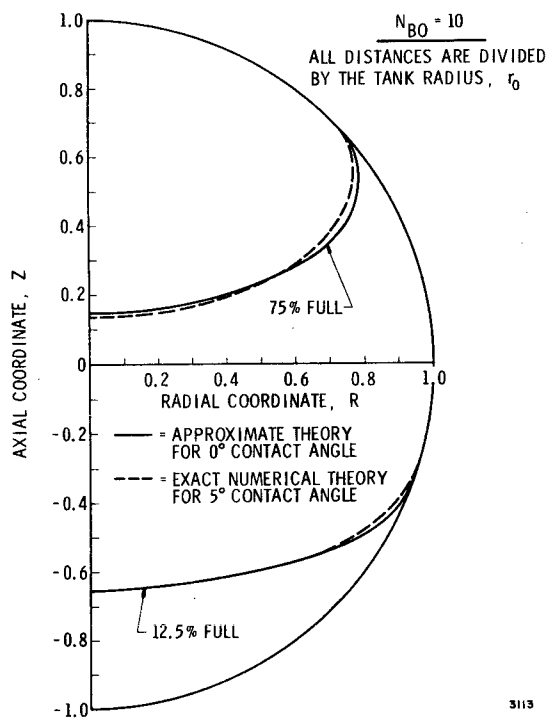
$$\frac{1}{\beta} = 1 + 0.168 B^2 N_{BO} \quad (19)$$

Furthermore, the curvature [Eq. (2)] of both F_1 and F_2 must be the same at $R = B$ in order to give a continuous pressure. Thus,

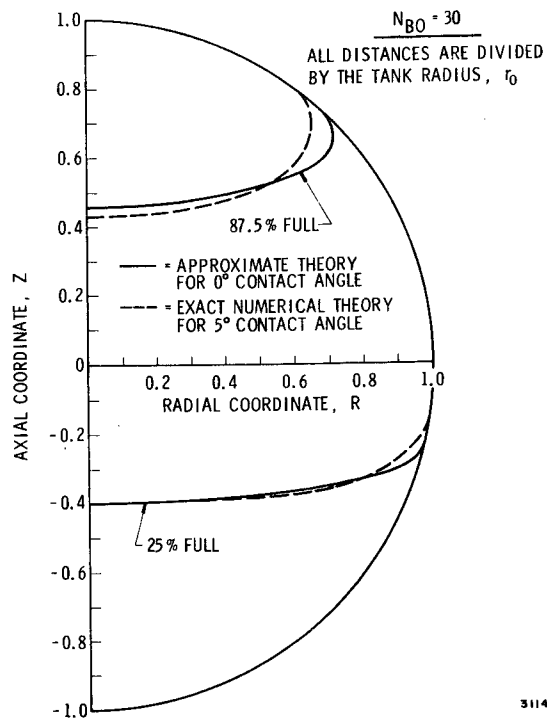
$$\mu^2 = \frac{1}{2} \beta^2 \quad (20)$$

These equations specify F_1 and F_2 for a bent-over free surface.

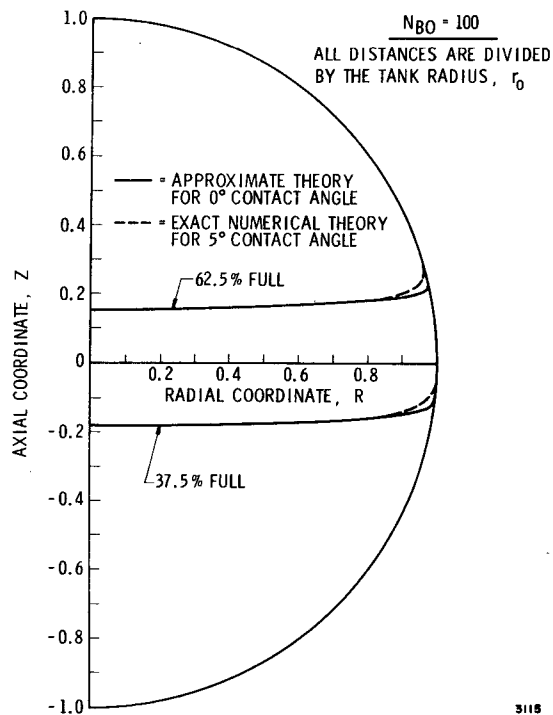
Comparisons of the free-surface shapes predicted by these equations to the exact shape given in Ref. 5 for a 5° contact angle, are shown in Figures 2a, 2b, and 2c for a spherical tank and various Bond numbers. The comparison is very good except for the case of a nearly full tank.



a. $N_{BO} = 10$, 75% and 12.5% Full



b. $N_{BO} = 30$, 87.5% and 25% Full



c. $N_{BO} = 100$, 62.5% and 37.5% Full

FIGURE 2. COMPARISON OF APPROXIMATE AND EXACT THEORIES

III. SLOSHING ANALYSIS

A. Basic Equations

The integral or variational form of the sloshing equations of motion can be obtained either from Hamilton's principle or by a direct integration of the differential equations of motion. In both cases, it is necessary that the "kinematic" boundary condition for the wave height be satisfied independently; that is, η and ϕ must satisfy the relation that

$$\frac{\partial \eta}{\partial t} = \frac{\partial \phi}{\partial z} - \frac{df}{dr} \left(\frac{\partial \phi}{\partial r} \right) = \frac{\partial \phi}{\partial n} \left[1 + \left(\frac{df}{dr} \right)^2 \right]^{1/2}, \quad z = f(r)$$

where η , the wave height, is measured vertically above the equilibrium free surface and $\partial \phi / \partial n$ is the fluid velocity normal to the free surface. This equation is nondimensionalized by assuming that $\phi = \bar{\phi}[r, \theta, z] \cos \omega t = (gr_o^3)^{1/2} \Phi[R, \theta, Z] \cos \Omega \tau$ and $\eta = \bar{\eta}[R, \theta] \sin \omega t = (r_o/\Omega) \epsilon[R, \theta] \sin \Omega \tau$, where $\Omega = \omega(r_o/g)^{1/2}$ is the nondimensional natural frequency and $\tau = t(g/r_o)^{1/2}$ is the nondimensional time. In nondimensional form, the above equation is thus

$$\epsilon = \partial \Phi / \partial Z - (dF/dR)(\partial \Phi / \partial R) = (\partial \Phi / \partial n) [1 + (dF/dR)^2]^{1/2}, \quad Z = F(R) \quad (21)$$

According to Hamilton's principle, the remaining equations of motion can be obtained by requiring that ϕ and η are such as to minimize the integral

$$I = \int_{t_1}^{t_2} (T - U) dt$$

where T is the kinetic energy of the liquid and U is the potential energy, including surface tension effects, and the integral is taken over one cycle of the motion. Following Satterlee and Reynolds [1], this integral, in nondimensional variables and after the integration over time is performed, is

$$I = \frac{1}{2} \Omega^2 \iiint_V (\nabla \Phi \cdot \nabla \Phi) R dR d\theta dZ - \frac{1}{2} \left(\frac{R_w \Gamma}{N_{BO}} \right) \int_0^{2\pi} \frac{\epsilon^2}{[1 + (dF/dR)^2]^{3/2}} \bigg|_{R=R_w} d\theta \\ - \frac{1}{2} \iint_{\mathcal{F}} \left(\frac{1}{N_{BO}} \left\{ \frac{(\partial \epsilon / \partial R)^2}{[1 + (dF/dR)^2]^{3/2}} + \frac{(\partial \epsilon / R \partial \theta)^2}{[1 + (dF/dR)^2]^{1/2}} \right\} + \epsilon^2 \right) R dR d\theta \quad (22)$$

where the first integral is taken over the entire volume V of the liquid, the second integral over the contact line $R = R_w$, and the third integral over the free surface \mathcal{F} . The authors of Ref. 1 apparently believed that Eq. (22) does not lead to the correct differential equations because, after formulating an integral similar to Eq. (22), they then use a different variational integral in their numerical work. However, Eq. (22) does in fact yield the correct equations, as will now be shown. By proceeding as shown by Hildebrand [7], the variation of Eq. (22) is

$$\delta I = \Omega^2 \iiint_V (\nabla \Phi \cdot \delta \nabla \Phi) dV - (R_w \Gamma / N_{BO}) \int_0^{2\pi} \frac{\epsilon \delta \epsilon}{[1 + (dF/dR)^2]^{3/2}} \bigg|_{R=R_w} d\theta \\ - \iint_{\mathcal{F}} \left(\frac{1}{N_{BO}} \left\{ \frac{(\partial \epsilon / \partial R) \delta (\partial \epsilon / \partial R)}{[1 + (dF/dR)^2]^{3/2}} + \frac{(\partial \epsilon / \partial \theta) \delta (\partial \epsilon / \partial \theta)}{R^2 [1 + (dF/dR)^2]^{1/2}} \right\} + \epsilon \delta \epsilon \right) R dR d\theta \quad (23)$$

Because $\delta(\nabla\Phi) = \nabla(\delta\Phi)$, the volume integral can be transformed by Green's theorem to give

$$\iiint_V (\nabla\Phi \cdot \nabla\delta\Phi) dV = - \iiint_V (\nabla^2\Phi) \delta\Phi dV + \iint_{\mathcal{F}} \left(\frac{\partial\Phi}{\partial n} \right) \delta\Phi d\mathcal{F} + \iint_{\mathcal{W}} \left(\frac{\partial\Phi}{\partial n} \right) \delta\Phi d\mathcal{W}$$

where the first surface integral is taken over the free surface \mathcal{F} and the second over the tank walls \mathcal{W} . The surface integrals in Eq. (23) are now integrated once by parts to give the following relations [7]:

$$\begin{aligned} \iint_{\mathcal{F}} \left\{ \frac{(\partial\epsilon/\partial R) \delta(\partial\epsilon/\partial R)}{[1 + (dF/dR)^2]^{3/2}} \right\} R dR d\theta &= \int_0^{2\pi} \left. \frac{R (\partial\epsilon/\partial R) \delta\epsilon}{[1 + (dF/dR)^2]^{3/2}} \right|_{R=0}^{R=R_w} d\theta \\ &- \iint_{\mathcal{F}} \frac{\partial}{R\partial R} \left\{ \frac{R (\partial\epsilon/\partial R)}{[1 + (dF/dR)^2]^{3/2}} \right\} \delta\epsilon R dR d\theta \end{aligned} \quad (24a)$$

and

$$\begin{aligned} \iint_{\mathcal{F}} \left\{ \frac{(\partial\epsilon/\partial\theta) \delta(\partial\epsilon/\partial\theta)}{R^2 [1 + (dF/dR)^2]^{1/2}} \right\} R dR d\theta &= \int_0^{R_w} \frac{1}{R^2} \left\{ \frac{(\partial\epsilon/\partial\theta) \delta\epsilon}{[1 + (dF/dR)^2]^{1/2}} \right\} \bigg|_{\theta=0}^{\theta=2\pi} R dR \\ &- \iint_{\mathcal{F}} \left\{ \frac{(\partial^2\epsilon/\partial\theta^2)}{R^2 [1 + (dF/dR)^2]^{1/2}} \right\} R dR d\theta \end{aligned} \quad (24b)$$

The first integral on the right in Eq. (24b) is equal to zero because $\delta\epsilon$ at $\theta = 0$ is the same as $\delta\epsilon$ at $\theta = 2\pi$; that is, $\delta\epsilon$ is continuous. Collecting terms,

$$\begin{aligned} \delta I &= -\Omega^2 \iiint_V (\nabla^2\Phi) \delta\Phi dV + \Omega^2 \iint_{\mathcal{W}} \left(\frac{\partial\Phi}{\partial n} \right) \delta\Phi d\mathcal{W} + \left(\frac{R_w}{N_{BO}} \right) \int_0^{2\pi} \left. \frac{[(\partial\epsilon/\partial R) - \Gamma\epsilon] \delta\epsilon}{[1 + (dF/dR)^2]^{3/2}} \right|_{R=R_w} d\theta \\ &+ \iint_{\mathcal{F}} \left[\frac{1}{N_{BO}} \left(\frac{\partial}{R\partial R} \left\{ \frac{R (\partial\epsilon/\partial R)}{[1 + (dF/dR)^2]^{3/2}} \right\} + \frac{\partial^2\epsilon/\partial\theta^2}{R^2 [1 + (dF/dR)^2]^{1/2}} - N_{BO}\epsilon \right) \delta\epsilon \right. \\ &\quad \left. + \Omega^2 \left(\frac{\partial\Phi}{\partial n} \right) \left\{ 1 + \left(\frac{dF}{dR} \right)^2 \right\}^{1/2} \delta\Phi \right] R dR d\theta \end{aligned} \quad (25)$$

where the fact that the element of area $d\mathcal{F}$ is $[1 + (dF/dR)^2]^{1/2} R dR d\theta$ has been used in the last term.

Because $\delta\Phi$ and $\delta\epsilon$ are completely arbitrary, δI can only be equal to zero (that is, the value of the integral can be minimized) if each of the integrals in Eq. (25) is separately equal to zero:

$$\nabla^2\Phi = 0 \quad \text{in the liquid volume, } V \quad (26)$$

$$\frac{\partial\Phi}{\partial n} = 0 \quad \text{on the tank walls, } Z = W(R) \quad (27)$$

and

$$\frac{\partial\epsilon}{\partial R} - \Gamma\epsilon = 0 \quad \text{on the contact line, } R = R_w \quad (28)$$

Equations (26), (27), and (28) are consequences of requiring that the first three integrals on the right-hand side of Eq. (25) be equal to zero. The last integral in Eq. (25) involves both $\delta\Phi$ and $\delta\epsilon$; since the relation between $\delta\Phi$ and $\delta\epsilon$ on the free surface is not known, setting the integrand in this term equal to zero does not lead to a useful result. But, if in the original variation, the volume integral is transformed in an alternative way as

$$\iiint_V (\nabla\Phi \cdot \nabla\delta\Phi) dV = - \iiint_V (\delta\nabla^2\Phi) \Phi dV + \iint_{\mathcal{F}} \left[\delta \left(\frac{\partial\Phi}{\partial n} \right) \right] \Phi dF + \iint_{\mathcal{W}} \left[\delta \left(\frac{\partial\Phi}{\partial n} \right) \right] \Phi dW \quad (29)$$

then a useful form does result. According to Eq. (26), the variation can be zero only if $\nabla^2\Phi = 0$; thus, we also have $\delta\nabla^2\Phi = 0$. Further, according to Eq. (27), $\partial\Phi/\partial n = 0$ on \mathcal{W} ; therefore, $\delta(\partial\Phi/\partial n) = 0$ on \mathcal{W} . And because $\partial\Phi/\partial n = \epsilon[1 + (dF/dR)^2]^{-1/2}$ on \mathcal{F} and $R dR d\theta = [1 + (dF/dR)^2]^{-1/2} d\mathcal{F}$, the surface integral over \mathcal{F} on the right-side of Eq. (29) reduces to $\iint_{\mathcal{F}} \Phi \delta\epsilon R dR d\theta$. Using this last relation and then proceeding with the rest of the manipulations as before, the variation of the integral in this alternative form is

$$\begin{aligned} \delta I = & -\Omega^2 \iiint_V [\delta\nabla^2\Phi] \Phi dV + \Omega^2 \iint_{\mathcal{W}} \left[\delta \left(\frac{\partial\Phi}{\partial n} \right) \right] \Phi dW + \left(\frac{R_w}{N_{BO}} \right) \int_0^{2\pi} \frac{[(\partial\epsilon/\partial R) - \Gamma\epsilon] \delta\epsilon}{[1 + (dF/dR)^2]^{3/2}} \Big|_{R=R_w} \cdot d\theta \\ & + \iint_{\mathcal{F}} \left(\frac{1}{N_{BO}} \left[\frac{\partial}{R\partial R} \left\{ \frac{R(\partial\epsilon/\partial R)}{[1 + (dF/dR)^2]^{3/2}} \right\} + \frac{\partial^2\epsilon/\partial\theta^2}{R^2 [1 + (dF/dR)^2]^{1/2}} \right] - \epsilon + \Omega^2\Phi \right) \delta\epsilon R dR d\theta \quad (30) \end{aligned}$$

Consequently, the only way that δI can equal zero is if in addition to requiring that Eqs. (26), (27), and (28) be satisfied, it is also required that

$$\frac{1}{N_{BO}} \left[\frac{\partial}{R\partial R} \left\{ \frac{R(\partial\epsilon/\partial R)}{[1 + (dF/dR)^2]^{3/2}} \right\} + \frac{\partial^2\epsilon/\partial\theta^2}{R^2 [1 + (dF/dR)^2]^{1/2}} \right] - \epsilon + \Omega^2\Phi = 0, \quad Z = F(R) \quad (31)$$

Eq. (31) is the last of the required sloshing equations of motion. Thus, any function Φ , with ϵ calculated from Φ by Eq. (21), that minimizes the integral Eq. (22) will also satisfy all of the sloshing equations of motion.

As mentioned previously, Satterlee and Reynolds [1] and Yeh [4] used a variational integral that was derived by a direct integration of Eqs. (26), (27), (28), and (31), with Eq. (21) as a required side condition. This procedure leads to

$$\begin{aligned} I = & \frac{1}{2} \Omega^2 \iiint_V (\nabla\Phi \cdot \nabla\Phi) dV - \frac{1}{2} (R_w \Gamma / N_{BO}) \int_0^{2\pi} \frac{\epsilon^2}{[1 + (dF/dR)^2]^{3/2}} \Big|_{R=R_w} \cdot d\theta \\ & + \frac{1}{2} \iint_{\mathcal{F}} \left[\frac{1}{N_{BO}} \left\{ \frac{(\partial\epsilon/\partial R)^2}{[1 + (dF/dR)^2]^{3/2}} + \frac{(\partial\epsilon/\partial\theta)^2}{R^2 [1 + (dF/dR)^2]^{1/2}} + \epsilon^2 \right\} R dR d\theta \right] \\ & - \Omega^2 \iint_{\mathcal{F}} (\epsilon\Phi) R dR d\theta \quad (32) \end{aligned}$$

Eq. (32) differs from Eq. (22) in the sign of the first surface integral and in the addition of the term $-\Omega^2 \iint_{\mathcal{F}} (\epsilon\Phi) R dR d\theta$. There is no evident physical significance to Eq. (32), but it does lead directly to the

differential equations of motion, which can be proved by repeating the procedure that yielded Eq. (25). In this case, all of the Eqs. (26), (27), (28), and (31) fall out at once, without further arguments or repeating the variation in an alternate form. For this reason, Eq. (32) may lead to a more rapid convergence of the sequence of trial functions for Φ to the true solution; thus, Eq. (32) or a similar formulation will be used in the present work.

Although Eq. (32) is suitable for use with a free surface that is not double-valued or bent over, the linearization of the equations with respect to ϵ breaks down at the point on a bent-over free surface where $dF/dR = \infty$ (i.e., at the point of vertical slope of the surface). At this point, $\epsilon = \infty$, according to Eq. (21), unless also $\partial\Phi/\partial R = 0$. But $\partial\Phi/\partial R = 0$ is not a realistic requirement unless the point where the slope is vertical is also the point where the free surface meets the wall; in this case $\partial\Phi/\partial R = \partial\Phi/\partial n$ does equal zero because the normal velocity at the wall must be zero. In general, however, $\epsilon = \infty$ and thus the second and higher powers of ϵ cannot be neglected in the equations. On the other hand, this prediction of an infinitely large wave height is simply a consequence of the way in which the wave height is defined. If instead of measuring ϵ vertically above F , ϵ is measured in the direction normal to F , as shown in Fig. 3, then Eq. (21) is replaced by

$$\epsilon = \partial\Phi/\partial n \quad \text{at } Z = F(R) \quad (33)$$

For this case, ϵ is always finite. (As will be seen presently, however, this definition of ϵ still leads to difficulties in the contact angle condition.) To be consistent, Eq. (32) also must be modified to account for the change in the definition of ϵ :

$$I = \frac{1}{2} \Omega^2 \iiint_V (\nabla\Phi \cdot \nabla\Phi) dV - \Omega^2 \iint_{\mathcal{F}} (\epsilon\Phi) d\mathcal{F} - \frac{1}{2} (R_w \Gamma' / N_{BO}) \int_0^{2\pi} \epsilon^2 \Big|_{R=R_w} d\theta + \iint_{\mathcal{F}} \left[\frac{1}{N_{BO}} \left\{ \frac{(\partial\epsilon/\partial R)^2}{1 + (dF/dR)^2} + \left(\frac{\partial\epsilon}{R\partial\theta} \right)^2 - G\epsilon^2 \right\} + \frac{\epsilon^2}{[1 + (dF/dR)^2]^{1/2}} \right] d\mathcal{F} \quad (34)$$

where

$$G = \frac{(d^2F/dR^2)^2}{[1 + (dF/dR)^2]^3} + \frac{(dF/dR)^2}{R^2 [1 + (dF/dR)^2]} \quad (35)$$

The double-valuedness in the analytical representations of Φ , F , and ϵ along the free surface can be removed by transforming the coordinate $R, \theta, Z = F(R)$ which locates a given point on the surface into the coordinate S, θ , where S is the arc-length along the surface from the point $R = Z = 0$ to the point in question. The transformation is

$$\frac{dS}{dR} = [1 + (dF/dR)^2]^{1/2}, \quad Z = F(R) \quad (36)$$

as shown in Fig. 3.

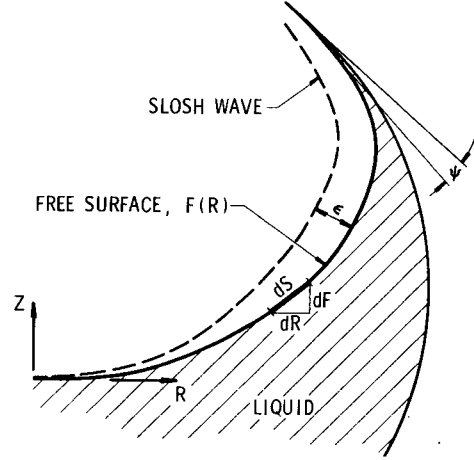


FIGURE 3. NORMAL-TANGENTIAL COORDINATE SYSTEM

The normal derivatives, $\partial\Phi/\partial n$, on the free surface and the tank walls can be evaluated by the relations

$$\frac{\partial\Phi}{\partial n} = \left[\frac{\partial\Phi}{\partial Z} - \left(\frac{dF}{dR} \right) \frac{\partial\Phi}{\partial R} \right] / [1 + (dF/dR)^2]^{1/2}, \quad Z = F(R) \quad (37a)$$

$$\frac{\partial\Phi}{\partial n} = - \left[\frac{\partial\Phi}{\partial Z} - \left(\frac{dW}{dR} \right) \frac{\partial\Phi}{\partial R} \right] / [1 + (dW/dR)^2]^{1/2}, \quad Z = W(R) \quad (37b)$$

where the change in sign is required because the positive normal direction must always point outward.

Finally, for numerical work, it is best to eliminate the volume integral in Eq. (34) by requiring that all of the assumed functions for Φ must satisfy $\nabla^2\Phi = 0$ identically. Then, Green's theorem shows that Eq. (34) reduces to

$$\begin{aligned} I = & \frac{1}{2} \Omega^2 \iint_{\mathcal{W}} \Phi \left(\frac{\partial\Phi}{\partial n} \right) d\mathcal{W} - \frac{1}{2} \Omega^2 \iint_{\mathcal{F}} \epsilon \Phi d\mathcal{F} - \frac{1}{2} \left(\frac{R_w \Gamma'}{N_{BO}} \right) \int_0^{2\pi} \epsilon^2 \bigg|_{R=R_w} d\theta \\ & + \iint_{\mathcal{F}} \left\{ \frac{1}{N_{BO}} \left[\frac{(\partial\epsilon/\partial R)^2}{1 + (dF/dR)^2} + \left(\frac{\partial\epsilon}{R\partial\theta} \right)^2 - G\epsilon^2 \right] + \frac{\epsilon^2}{[1 + (dF/dR)^2]^{1/2}} \right\} d\mathcal{F} \end{aligned} \quad (38)$$

An analogous equation can be written when ϵ is measured vertically above F .

B. Contact Line Condition

The contact line condition implied by Eq. (22) or (32) is

$$\frac{\partial\epsilon}{\partial R} = \Gamma\epsilon \quad \text{at } R = R_w$$

and the one implied by Eq. (34) or (38) is

$$\frac{\partial\epsilon}{\partial S} = \Gamma'\epsilon \quad \text{at } R = R_w$$

For the “no stick” condition (the liquid slides freely along the wall) of interest here, Γ and Γ' are functions only of the tank geometry and the free-surface shape, and the magnitude of Γ or Γ' is picked so that the contact angle that the wave makes with the wall always is equal to the static contact angle. *But, Γ or Γ' cannot be calculated unambiguously because it is impossible to define a wave height ϵ at the wall in an unambiguous manner.* This is demonstrated in Fig. 4, which shows the point of the wave contacting the wall cannot be correlated in a definitive way with any point on the static-free surface, either when ϵ is measured vertically above F or when measured normal to it. As can be seen, various values of Γ or Γ' are possible, depending upon what kind of approximations are used. The approximation used by Concus, et al. [5] and by Chu [6] for the normal direction definition of ϵ (Fig. 7c) leads to

$$\Gamma' = \frac{1}{\sin\psi} \left\{ \frac{d^2 W/dR^2}{[1 + (dW/dR)^2]^{3/2}} - \frac{\cos\psi (d^2 F/dR^2)}{[1 + (dF/dR)^2]^{3/2}} \right\}, \quad R = R_w \quad (39)$$

and thus, $\Gamma' = \infty$ when $\psi = 0$. This requires that $\epsilon = 0$ at $R = R_w$ for otherwise $\partial\epsilon/\partial S = \infty$, which implies that there is a jump in the wave height at the contact line.

Now, $\partial\Phi/\partial n = 0$ all along the walls; and, for the case $\psi = 0$, $\partial\Phi/\partial n$ on the wall at $R = R_w$ also equals $\partial\Phi/\partial n$ on the free surface at $R = R_w$. Therefore, $\partial\Phi/\partial n$ on the free surface at the contact line also is zero; but, because $\epsilon = \partial\Phi/\partial n$ on the contact line (and all over the free surface), it can be concluded that $\epsilon = 0$ on the contact line, which agrees with the first conclusion concerning ϵ at $R = R_w$. In fact, $\epsilon = 0$ at $R = R_w$ is the "correct" contact condition when $\psi = 0$ and the equation $\partial\epsilon/\partial S = \Gamma'\epsilon$ is essentially redundant. But, the fact that $\epsilon = 0$ at $R = R_w$ requires analytically that the liquid is not allowed to move away from the equilibrium contact line; in other words, the linearized slosh wave is "stuck" to the contact line. This is probably not true in practice but is just a mathematical consequence of both the linearization of the equations and of the ambiguity in defining a proper wave height at the wall.

In the finite-difference numerical analyses presented in Refs. 5 and 6, the contact angle ψ was always equal to a non-zero value (usually 5 degrees). Hence, in these studies, $\Gamma' \neq \infty$ and $\epsilon \neq 0$ at the contact point. (Further, $\partial\Phi/\partial n$ on \mathcal{F} at the contact point is not equal to $\partial\Phi/\partial n$ on \mathcal{W} at the contact point, and thus ϵ does not have to be zero at $R = R_w$.) It might be possible, therefore, to approach the case $\psi \equiv 0$ numerically in order to determine if the numerical solutions converge to a definite value as $\psi \rightarrow 0$. In this regard, however, Chu [6] noticed a sensitivity in his results to changes in the value of ψ or Γ' for small values of ψ . In the absence of evidence to the contrary, it seems likely that the definition of Γ' in Eq. (39) is *not* sufficient to eliminate the mathematical difficulties when $\psi = 0$, and, for this reason, it might not be accurate to extrapolate the results presented in Refs. 5 and 6 to the case $\psi = 0$ unless the extrapolations are verified by accurate experiments.

Measuring ϵ vertically above F also leads, in general, to the result that $\epsilon = 0$ at the contact line when $\psi = 0$. The only exception to the condition that $\epsilon = 0$ at $R = R_w$ is the case for which the free surface at the contact line has a vertical tangent, as in a cylindrical tank; for this case, the vertical wave height *can* be defined unambiguously at the contact line. (Mathematically, $dF/dR = \infty$ at $R = R_w$, and so $\epsilon = (\partial\Phi/\partial n)[1 + (dF/dR)^2]^{1/2} = 0 \times \infty$, which is undefined. Thus, ϵ is not necessarily zero at $R = R_w$, and, in fact, the correct contact line condition is $\partial\epsilon/\partial R = 0$ at $R = R_w$.)

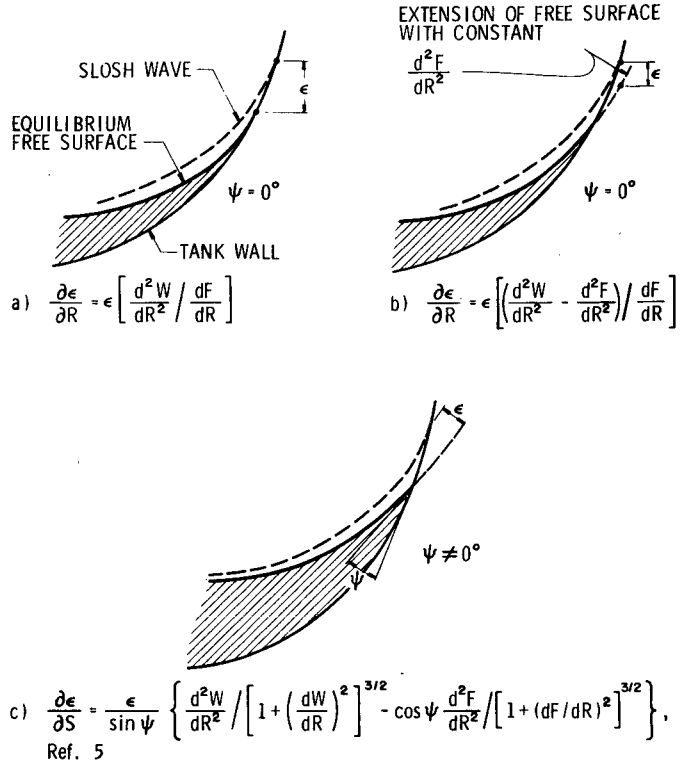


FIGURE 4. VARIOUS CONTACT LINE CONDITIONS

IV. SOLUTION OF EQUATIONS

A. Rayleigh-Ritz Technique

The form of Rayleigh-Ritz technique used here to solve the variational integral involves assuming a set of functions $\Phi_n(R, \theta, Z)$, $n = 1, 2, 3, \dots, N$, each of which satisfies $\nabla^2 \Phi_n = 0$. Then, the velocity potential is written as the sum

$$\Phi(R, \theta, Z) = \sum_{n=1}^N \alpha_n \Phi_n(R, \theta, Z)$$

where the constants α_n are to be determined. The wave height ϵ , calculated by Eq. (21) or Eq. (27), is

$$\epsilon(R, \theta) = \sum_{n=1}^N \alpha_n \epsilon_n(R, \theta)$$

These expressions are substituted into the variational integral, Eq. (38), and the various definite integrals are computed numerically. The result is

$$I = \sum_{n=1}^N \sum_{m=1}^N \alpha_n \alpha_m (B_{nm} - \Omega^2 A_{nm})$$

where the constants B_{nm} and A_{nm} are the values of the definite integrals of Φ_n , Φ_m , ϵ_n , and ϵ_m and their derivatives in Eq. (38). The value of I is minimized by picking the values of α_n such that

$$\frac{\partial I}{\partial \alpha_n} = \sum_{m=1}^N [B_{nm} + B_{mn} - \Omega^2 (A_{nm} + A_{mn})] \alpha_m = 0, \quad n = 1, 2, 3, \dots, N$$

In matrix form, this equation is

$$[B + B^T] [\alpha] - \Omega^2 [A + A^T] [\alpha] = 0 \quad (40)$$

The two solutions of Eq. (40) are $[\alpha] = 0$, which means the liquid has no motion at all, a solution which is not of interest here, and

$$|[B + B^T] - \Omega^2 [A + A^T]| = 0 \quad (41)$$

Eq. (41) represents a standard eigenvalue problem, and the values of $\Omega = \Omega_n$ which allow the determinant in Eq. (41) to be equal to zero are the natural frequencies Ω_n , or slosh frequencies, of the problem. Once the Ω_n are known (there are N of them), the constants α_n , which are the eigenvectors, can be computed with the aid of Eq. (40).

In the limit as $N \rightarrow \infty$, Φ and ϵ , when determined in the above way, satisfy the boundary conditions, Eqs. (27), (28), and (30); also Φ satisfies the incompressibility condition $\nabla^2 \Phi = 0$ [Eq. (26)]. Thus, Φ is the true velocity potential of the low-gravity sloshing problem, and the slosh mode shapes, forces, moments, etc. can be calculated.

B. Trial Functions and Results

To make the Rayleigh-Ritz technique feasible, it is usually necessary to pick trial functions Φ_n that "suit" the problem. Two different sets of functions were evaluated during the present work. The first was the set of polynomials used by Rattaya [3]:

$$\Phi_n(R, \theta, Z) = \cos \theta \sum_{k=1,3,\dots,n}^n a_k^{(n)} R^k Z^{n-k} \quad (41)$$

where, in order to satisfy $\nabla^2 \Phi_n = 0$, it is necessary that

$$a_k^{(n)} = - \left[\frac{(n-k+2)(n-k+1)}{k^2-1} \right] a_{k-2}^{(n)}, \quad k=3,5,\dots,n$$

and

$$a_1^{(n)} = 1 \quad \text{for all } n$$

Rattaya reported excellent results using Eq. (41), with $N \leq 12$, in his analysis of sloshing in ellipsoidal tanks, which neglected low-gravity effects. However, these functions gave very poor results during the present study and were abandoned rather early.*

The second set of functions used in the present study were those that describe sloshing in a cylindrical tank:

$$\Phi_n(R, \theta, Z) = \cos \theta \cdot J_1(\lambda_n R) \cdot \left\{ \frac{\cosh [\lambda_n(Z + H + L)]}{\cosh [\lambda_n(F_{\max} + H + L)]} \right\} \quad (42)$$

where $F_{\max} = F(R_w)$.

The constant λ_m in each Φ_m was picked so that Φ_m satisfied in some sense the boundary condition $\partial\Phi/\partial n = 0$ on the tank walls; this should improve the rate of convergence of $\sum \alpha_m \Phi_m$ to the true Φ . One method that was tried was to use the value of λ_m that made $\partial\Phi_m/\partial R = 0$ at $R = 1$. Thus, with this method, the normal velocity was zero over all the cylindrical surface, $R = 1$, $L - H \geq Z \geq -L - H$, $0 \leq \theta \leq 2\pi$, and $0 \leq R \leq 1$, $Z = -L - H$, $0 \leq \theta \leq 2\pi$, which bounds the actual tank; this is the technique suggested by Moiseev and Petrov [8]. (Note, however, that the assumed contact line condition $\epsilon = 0$, which should be satisfied by the sum $\sum \alpha_m \epsilon_m$, is not satisfied by each ϵ_m individually when computed in this way; the reason for this is that the condition used to calculate λ_n does not insure that $\partial\Phi_m/\partial n = 0$ at the contact point.) Table I gives representative values of Ω_1 for a spherical tank that were calculated using these λ_n , for the case $N_{BO} = 100$ and a free surface that is not bent over. As can be seen, the comparison with the present results and those given by Rattaya [3] (for $N_{BO} = \infty$) are fairly close; with further refinement in the numerical work, it is believed that the comparison would be even closer.

TABLE I. VARIATION OF Ω_1 AS A FUNCTION OF TANK FILLING AND NUMBER OF TERMS IN APPROXIMATING SERIES FOR Φ . $N_{BO} = 100$

Liquid Volume	N	Ω_1	Ω_1 , Ref. 3
47.2%	5	1.274	1.230
	12	1.276	
35%	5	1.239	1.185
	12	1.239	
30%	5	1.231	1.160
	12	1.231	
25%	5	1.226	1.140
	12	1.226	
20%	5	1.225	1.125
	12	1.225	
15%	5	1.230	1.100
	12	1.230	

*Because Rattaya neglected surface tension and curvature effects, he was able to include the boundary condition Eq. (21) in his variational integral. Thus, for any finite value of N_{BO} , his integral and the present one cannot be made to be identical.

The second method was to use the value of λ_m in Eq. (42) that made $\partial\Phi_m/\partial n = 0$ at the contact line; this automatically forced each ϵ_m to be equal to zero at the contact line, which thus identically satisfied one more of the boundary conditions. The results using this method were quite similar to the results presented in Table I.

For bent-over free surfaces, neither method of picking λ_m seemed to give satisfactory results. As an example, the case $N_{BO} = 100$ for a 70% full spherical tank resulted in $\Omega_1 = 1.797$ for $\psi = 0^\circ$ whereas, according to Refs. 5 or 6, the correct result is about $\Omega_1 = 1.34$ when $\psi = 5^\circ$. After many more test cases and manipulations of the trial functions Φ_m , with no further improvement in the prediction of Ω_1 , it was concluded that either (1) a suitable set of functions Φ_m had not been discovered* or else (2) the boundary condition that $\epsilon_m = 0$ at $R = R_w$ forced the frequency to be too large because of the added “stiffness” given to the free surface as a result of the “stuck” contact line. A third alternative is that the present result for $\psi = 0^\circ$ is correct, or could be made so with further refinement of the technique, so that therefore the difference between the present Ω_1 and the result given in Ref. 5 is due to ψ being 5° in Ref. 5. This alternative would be a likely explanation if the numerical technique used in Refs. 5 or 6 does not converge to a definite result as $\psi \rightarrow 0^\circ$. However, it was not feasible to evaluate the numerical convergence of these methods during this project.

*Another obvious set is Legendre polynomials.

V. CONCLUSIONS

It has been shown that Hamilton's principle leads to a variational form of the sloshing equation which is equivalent to the usual differential equations. A second form of the variational integral, which may be more convenient to use in numerical work, was derived by direct integration of the differential equations and boundary conditions and was used in the subsequent work.

The "contact line condition" implicit in the variational form of the sloshing equations (or assumed in the differential equation form) was shown to be ambiguous for the case of a zero-degree contact angle. The ambiguity is a result of both the linearization of the equations with respect to the wave height and the impossibility of mathematically defining the slosh height at the walls of an ellipsoidal tank. Although the ambiguity does not appear to be serious for non-zero contact angles, it is believed to be a critical limitation in the analysis of bent-over free surfaces with a zero-degree contact angle.

Numerical results of sloshing in ellipsoidal tanks for free surfaces that are not bent over (tanks less than half-full) compare well with previous work. For bent-over surfaces, however, the computed natural frequencies were considerably larger than those computed previously for a contact angle of 5 degrees. The discrepancy is probably the result of the contact line condition difficulty mentioned above which, for a zero-degree contact angle, implies analytically that the slosh wave is "stuck" to the contact line. A satisfactory resolution of the contact line difficulty was not obtained.

VI. REFERENCES

1. Satterlee, H. M. and Reynolds, W. C., "The Dynamics of the Free Liquid Surface in Cylindrical Containers under Strong Capillary and Weak Gravity Conditions," Technical Report LG-2, Grant NSF-G20090, Department of Mechanical Engineering, Stanford University, May 1, 1964.
2. Dodge, F. T. and Garza, L. R., "Experimental and Theoretical Studies of Liquid Sloshing at Simulated Low Gravity," *Trans. ASME, J. Applied Mechanics*, **34**, September 1967, pp. 555-561. (Also, Technical Report No. 2, Contract NAS8-20290, Southwest Research Institute, October 20, 1966.)
3. Rattaya, J. V., "Sloshing of Liquids in Axisymmetric Ellipsoidal Containers," AIAA Paper 65-114, January 1965.
4. Yeh, G. C. K., "Free and Forced Oscillations of a Liquid in an Axisymmetric Tank at Low-Gravity Environments," *Trans. ASME, J. Applied Mechanics*, **34**, March 1967, pp. 23-28.
5. Concus, P., Crane, G. E., and Satterlee, H. M., "Small Amplitude Lateral Sloshing in Spheroidal Containers Under Low Gravitational Conditions," Final Report, Contract NAS3-9704, Lockheed Missiles and Space Corporation, February 1969.
6. Chu, W.-H., "A Theory for Low-Gravity Fuel Sloshing in an Arbitrary Axisymmetric Rigid Tank," *Trans. ASME, J. Applied Mechanics*, **37**, September 1970, pp. 828-837. (Also, Technical Reports No. 8, April 1969, and No. 10, August 1970, Contract NAS8-20290, Southwest Research Institute.)
7. Hildebrand, F. B., **Methods of Applied Mathematics**, Chapter 2, Prentice-Hall, Inc., Englewood Cliffs, New Jersey, 1963.
8. Moiseev, N. N. and Petrov, A. A., "The Calculation of Free Oscillations of a Liquid in a Motionless Container" in **Advances in Applied Mechanics 1966**, pp. 91-153, Academic Press, New York, 1966.

APPENDIX

Summary of

"Low Gravity Sloshing in Rectangular Tanks"

by

**Franklin T. Dodge
Luis R. Garza**

**Technical Report No. 1
Contract NAS8-24022**

January 1970

Liquid sloshing in rectangular tanks was studied theoretically and experimentally under low Bond number conditions. The static-free surface shape was computed accurately by an approximate technique, and the results were used in the equations of motion for the fluid to determine the sloshing parameters. The sloshing equations were solved by Galerkin's method. The natural frequency parameter was found to increase, and the equivalent slob mass to decrease, under low Bond number conditions. Nonlinearities in the experimental results prevented a close comparison of theory and test, but the trends of both were similar. Exploratory tests with square tanks showed that nonlinear effects prevailed here also, even for large Bond numbers.

Figures A-1, A-2, and A-3 show the comparison of test and theory, for rectangular tanks having a width-to-thickness ratio of 10.

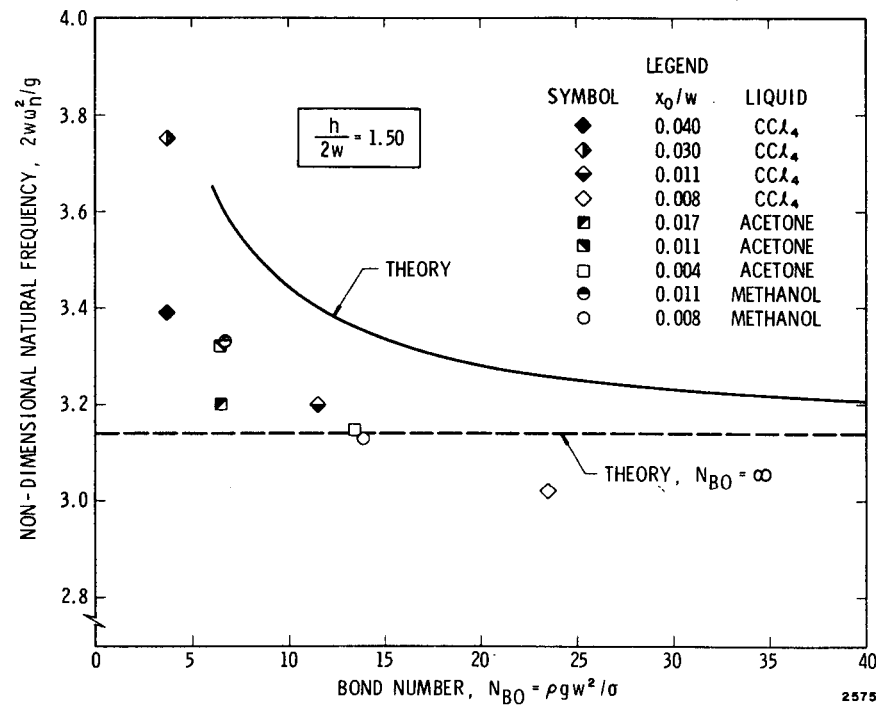


FIGURE A-1. NATURAL FREQUENCY VS N_{BO} FOR DEPTH RATIO OF 1.5

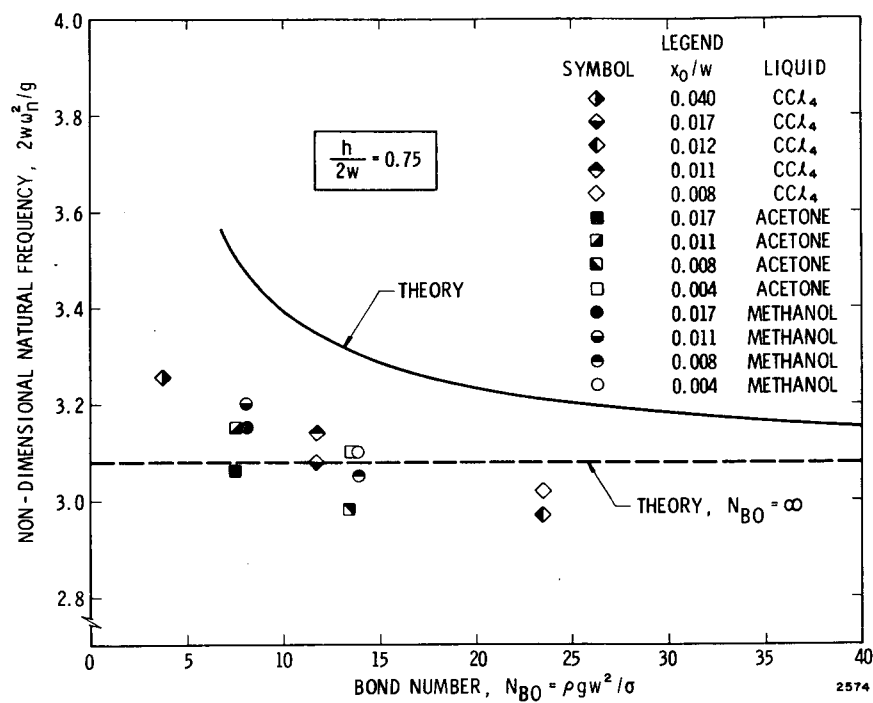


FIGURE A-2. NATURAL FREQUENCY VS N_{BO} , FOR DEPTH RATIO OF 0.75

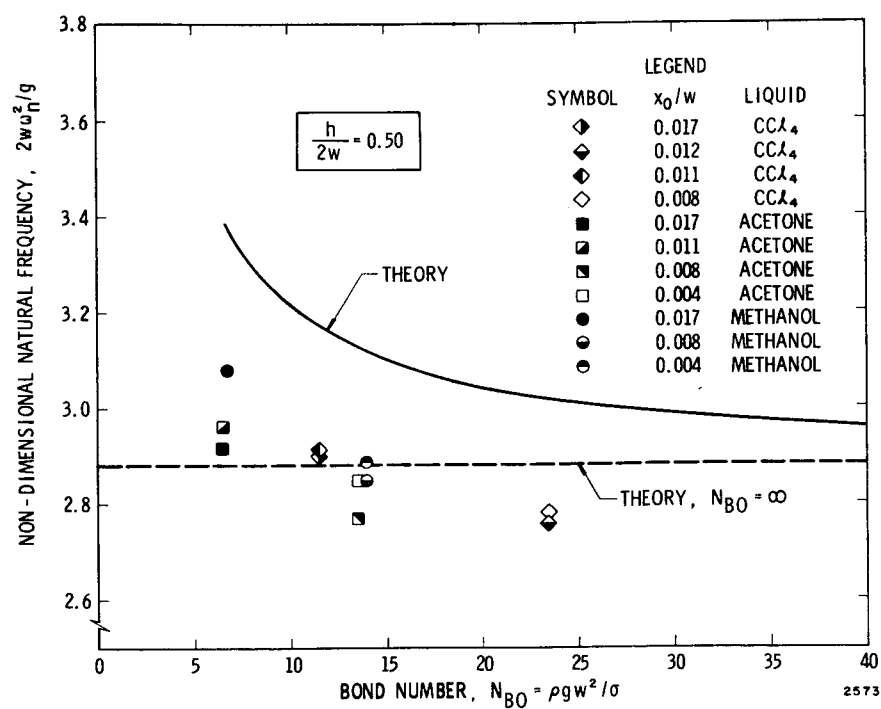


FIGURE A-3. NATURAL FREQUENCY VS N_{BO} , FOR DEPTH RATIO OF 0.50